Finance and Economics Discussion Series

Federal Reserve Board, Washington, D.C.
ISSN 1936-2854 (Print)
ISSN 2767-3898 (Online)

Trend-Cycle Decomposition and Forecasting Using Bayesian Multivariate Unobserved Components

Mohammad R. Jahan-Parvar, Charles Knipp, and Paweł J. Szerszeń

2024-100

Please cite this paper as:
Jahan-Parvar, Mohammad R., Charles Knipp, and Paweł J. Szerszeń (2024). "Trend-Cycle Decomposition and Forecasting Using Bayesian Multivariate Unobserved Components," Finance and Economics Discussion Series 2024-100. Washington: Board of Governors of the Federal Reserve System, https://doi.org/10.17016/FEDS.2024.100.

Trend-Cycle Decomposition and Forecasting Using Bayesian Multivariate Unobserved Components

Mohammad R. Jahan-Parvar Charles Knipp Paweł J. Szerszeń*

September 13, 2024

Abstract

We propose a generalized multivariate unobserved components model to decompose macroeconomic data into trend and cyclical components. We then forecast the series using Bayesian methods. We document that a fully Bayesian estimation, that accounts for state and parameter uncertainty, consistently dominates out-of-sample forecasts produced by alternative multivariate and univariate models. In addition, allowing for stochastic volatility components in variables improves forecasts. To address data limitations, we exploit cross-sectional information, use the commonalities across variables, and account for both parameter and state uncertainty. Finally, we find that an optimally pooled univariate model outperforms individual univariate specifications, and performs generally closer to the benchmark model.

JEL Classification: C11, C22, C32, C53.

Keywords: Bayesian estimation, Maximum likelihood estimation, Online forecasting, Out-of-sample forecasting, Parameter uncertainty, Sequential Monte Carlo methods, Trend-cycle decomposition.

*All authors are affiliated with the Federal Reserve Board of Governors. Please direct correspondence to Paweł J. Szerszeń (pawel.j.szerszen@frb.gov). We are grateful to seminar participants at the Federal Reserve Board of Governors, CFE 2023 conference, as well as Behzad Diba, Ali Habibnia, and Irina Panovska for conversations and comments. The analysis and conclusions are those of the authors, and do not reflect the views of other members of the research staff or the Board of Governors.

1 Introduction

A central problem in empirical econometrics is decomposing macroeconomic or financial time-series into long-run trends and cyclical components. Often, the econometrician wishes to forecast these components as they are of paramount research or policy importance. Important examples include the congressional budget office's (CBO) estimates of the output gap and potential output, often used for budgetary projections and debt sustainability studies (see Shackleton, 2018).

Univariate trend-cycle decomposition methods have a long history in applied econometrics.[1] However, current research increasingly requires decomposition of multivariate systems, often using information embedded in several variables and thus exploiting the cross-sectional variations, to extract the common trend and cyclical components. Exploiting these cross-sectional variations is a practical solution to overcome deficiencies in data, for example, relatively short time-series available for macroeconomic or financial research or policy making. Studies such as Creal, Koopman and Zivot (2010) in a partially estimated Bayesian smoother setting, González-Astudillo (2019a,b) within the unobserved component framework, Li and Koopman (2021) in state-space simulated maximum likelihood (SMLE) setting, and Barigozzi and Luciani (2023) using a dynamic factor model (DFM) set up, exploit different aspects of cross-sectional variations and recover trend and cyclical components of macroeconomic time-series. In this study, we use recent developments, such as Chopin, Jacob and Papaspiliopoulos (2013) sequential Monte Carlo and Andrieu, Doucet and Holenstein (2010) particle MCMC methods, and develop a continuously re-estimated Bayesian, online, trend-cycle decomposition and forecasting method that, by construction, avoids the look-ahead bias present in studies that rely on a smoother, such as Creal et al. (2010). In a related literature, Dobrev, Hansen and Szerszen (2022) also rely on online estimation to guard against data outliers using Randomized Missing Data approach for estimation of univariate UC models in forecasting inflation.

We recover trend and cyclical components of U.S. output (measured by real GDP), unemployment, and personal consumption expenditure (PCE) inflation, in a sample that includes the 2008-2009 global financial crisis (GFC), the COVID-19 pandemic, and the recent inflationary period. We show that our proposed model outperforms a host of alternative multivariate and univariate models, in both estimation and forecasting. We find that the following ingredients are essential to deliver the model's success:

- A fully estimated stochastic volatility (SV) component across all series modeled to induce estimation and forecasting flexibility, especially over periods of abrupt change, such as the COVID-19 pandemic. Indeed, Clark (2011) implements a Bayesian vector autoregression

[1] Among them, we note Hodrick and Prescott (1997), Baxter and King (1999) band-pass, and Hamilton (2018) filters, as well as unobserved component (UC) methods popularized by Stock and Watson (2007) and used by many others, which are among those that we focus in this study.

(BVAR) model featuring SV components and documents notable real-time forecast improvements of U.S. macroeconomic quantities.

- Fully accounting for both parameter and state uncertainty, through using filtering instead of smoother or (S)MLE methods. Moreover, using a filtering approach avoids the look-ahead bias problems inherent in smoother-based estimation (as in Panovska and Ramamurthy, 2022, Li and Koopman, 2021 or Clark, 2011), that use the full sample.[2] We note that using the entire sample (as in smoothing exercises) assumes access to future information that limits the appeal of such estimated models for policy making.

- Taking the commonalities and correlations across various time-series seriously, and putting every effort to use the cross-section of modeled time series to overcome generally short samples. An example of this approach in the literature is Panovska and Ramamurthy (2022) study, that uses learning about inflation to improve output gap estimation in a UC framework. We note that, as shown later in the paper, ignoring any of these components as in Stock and Watson (2007), Grant and Chan (2017), and Kamber et al. (2018) univariate studies or Creal et al. (2010) multivariate but less flexible and partially calibrated specification, leads to non-negligible underestimation of gaps.

- We show that when using univariate models, an optimally pooled model (following Amisano and Geweke, 2017) outperforms individual constituent models.

We document that the benchmark model in the paper, that could be viewed as a fully estimated version of Creal et al. (2010) with stochastic volatility components present in all series, and unrestricted estimation of volatility-of-volatility parameters, is easy to use in forecasting exercises, computationally feasible, avoids many pitfalls of earlier studies, and in comparison with DFM studies, generates very good out-of-sample forecasts using a parsimonious model. Our study explicitly incorporates relevant stylized facts about the United States macroeconomic data (comovements, nonstationarity, and the slow drift in long-run output growth over time). The method used in this study is a single-step procedure that does not require stationarity, cointegration, or partial integration among time-series variables used to identify potential common trends. However, we note that ours is a general estimation method suitable for various macroeconomic and financial time-series estimation, and is not tailored for the specific application presented in the paper.

Figure 1 highlights some important contributions of the study. The top row displays the cyclical components extracted from U.S. output, unemployment, and PCE inflation. The CBO produces highly influential forecasts of cyclical components for GDP and unemployment often called output and unemployment gaps, respectively, on a regular basis (quarterly for GDP and monthly for

[2] In comparison to Clark (2011)'s BVAR method, our method imposes less stringent structures on variables and allows for direct trend-cycle decomposition.

unemployment rate). We plot these forecasts as blue dotted lines in the top panel of the figure. The shaded areas represent 99, 95, and 75% credible intervals for cyclical components recovered through application of the benchmark method to the series. The choice of these credible intervals are similar but more stringent than those reported by Barigozzi and Luciani (2023). It is clear that CBO gap estimates generally fall within the 95% credible intervals of ours. Notable exceptions to this pattern are large spikes in output and unemployment gaps during the COVID-19 pandemic, and the recovery from large spike in the unemployment gap following the GFC, where our estimates show a smaller rise compared to CBO's. The bottom panel reports the extracted stochastic trends (solid lines) and data points (black dashed lines) for the same series.

Figure 1: Data and decomposition results

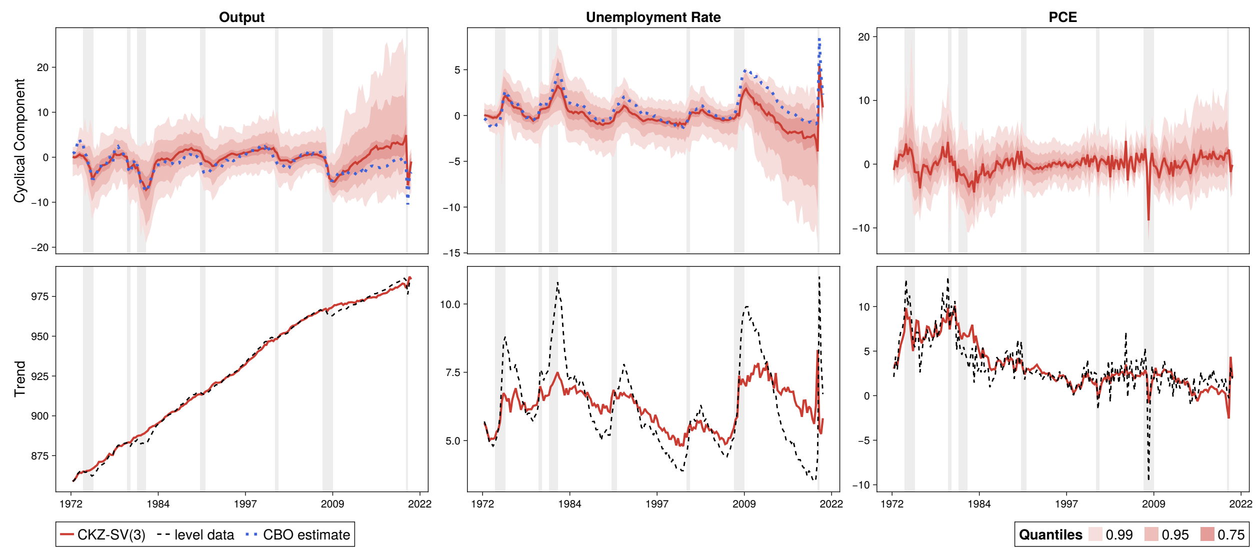

The figure displays the cyclical components of output, unemployment, and personal consumption expenditure on the top row, and their respective trends and raw data on the bottom row. For the cyclical components, the blue dotted line is the CBO estimate, while the solid line is our estimate. The shaded areas around our estimate are 75, 90, and 95% confidence bands, respectively. On the bottom row, solid lines represent the extracted stochastic trends and dashed black lines represent the data. All data are from FRED data bank, maintained by the Federal Reserve Bank of St. Louis.

We follow a statistical approach in recovering trend and cyclical components of macroeconomic time-series.[3] However, our estimation results yield gaps that are close to CBO's, that follow a more involved production function-based approach (see Shackleton, 2018). Thus, our study at least partially bridges an existing gap in the literature. Moreover, given the relative simplicity of our model and estimation procedures, these estimates are easy to update in real time. In comparison, New-Keynesian estimation of gaps (as in Justiniano et al., 2013) or DFM-based methods usually require more careful treatment of variables. In DFM's case, the number of variables that feed into

[3] While we use a statistical model, we exploit intuition from economic theory and reduced form estimations to model dependencies between variables.

the forecasting exercise is typically large, and estimated DSGE models used in New-Keynesian gap extraction tend to be sensitive to both modeling assumptions and data samples used.

The rest of the paper proceeds as follows. In Section 2 we discuss the data used in the estimations for the selected macroeconomic data series. In Section 3 we discuss the estimated models with an emphasis on the preferred benchmark model, the SMC^2 algorithm, and the online forecasting approach. In Section 4 we present our empirical findings, including comparisons between the benchmark model, alternative multivariate models, and alternative univariate models, and other ancillary results. Section 5 concludes.

2 Data

As mentioned in the introduction, we are interested in recovering the cyclical components of output and unemployment, and study their interactions with inflation. To this end, we use data from FRED database maintained by the Federal Reserve Bank of St. Louis to collect the following variables: 1) annualized, seasonally adjusted, quarterly, real gross domestic product (henceforth, GDP) in billions of chained 2012 dollars; 2) seasonally adjusted monthly unemployment rate (henceforth, UNRATE), that represents the number of unemployed as a percentage of the labor force (United States civilian and non-institutionalized residents 16 years of age and older); and 3) the monthly core personal consumption expenditures (henceforth, PCE) price index.

We use logarithmic values of real GDP (in levels) following the example of, among others, Kamber et al. (2018). The GDP sample spans the first quarter of 1960 to the first quarter of 2023. Monthly measures of inflation are based on the price index for PCE. Inflation rates are computed as annualized log-changes in monthly PCE price index. We consider PCE inflation for two important reasons. First, PCE inflation is the Federal Reserve's preferred inflation measure; Federal Reserve's longer-run inflation objectives are stated in terms of this measure. Second, PCE's historical data has been revised to reflect methodology changes over time, thus reducing concerns about instabilities that such changes might induce. PCE price index and unemployment samples span January 1960 to April 2023. In our multivariate studies, we use end-of-the-quarter values for PCE inflation and unemployment.

3 Methodology

3.1 The benchmark model

In this section we define our preferred trend-cycle decomposition, denoted as CKZ-SV, based on Harvey and Trimbur (2003) and further generalized to multivariate case following Creal et al. (2010). We extend the model by Creal et al. (2010) and allow for stochastic volatilities in all studied variables. We also unrestrict and estimate volatility of volatility parameters.

The model decomposes each series $y_{i,t}$ for $i \in 1,2,3$ (respectively PCE, unemployment and GDP) into trend $x_{i,t}$, the band-pass type common stochastic cycle $\psi_t^{(q)}$ and individual idiosyncratic cyclical (irregular and *i.i.d.*) components $\eta_{i,t}$:

$$\begin{aligned} y_{i,t} &= x_{i,t} + \delta_i \cos(\xi_i \lambda)\psi_t^{(q)} + \delta_i \sin(\xi_i \lambda)\psi_t^{+(q)} + \eta_{i,t} && (1) \\ x_{i,t+1} &= x_{i,t} + \mu_i + \varepsilon_{i,t} && (2) \end{aligned}$$

where

$$\begin{aligned} \eta_{i,t} &\sim N(0, \sigma^2_{i,t,\eta}) && (3) \\ \varepsilon_{i,t} &\sim N(0, \sigma^2_{i,t,\varepsilon}) && (4) \end{aligned}$$

are the idiosyncratic trend and idiosyncratic cyclical components, respectively. The coefficient ξ_i controls the shift in time of the common cycle component for the series i, while the parameter δ_i controls the scale of the cycle. We pick the PCE series $i = 1$ (PCE), to be the numeraire and hence set $\delta_1 = 1$ and $\xi_1 = 0$. so that the scale and shift of the common cycle is measured with respect to the PCE series. The coefficient λ measures the length of the cycle given by $2\pi/\lambda$.

We model the volatilities of $\eta_{i,t}$ and $\varepsilon_{i,t}$ to be stochastic but restrict our specification to two regimes due to data limitations stemming from the relatively short quarterly data sets

$$\begin{aligned} \sigma^2_{i,t,z} &= \exp(h_{i,t,z}) && (5) \\ h_{i,t+1,z} &= h_{i,t,z} + \gamma_{i,t,z} \qquad \gamma_{i,t,z} \sim N(0, K^2_{i,t,z}) && (6) \end{aligned}$$

where z denotes either η or ε and where the regime switches are defined by

$$K_{i,t,z} = \begin{cases} K_z^{(1)} & \text{with probability } p \\ K_z^{(2)} = 0 & \text{with probability } 1-p \end{cases} \tag{7}$$

with the first regime denoting the high-volatility regime. Due to data limitations we assume that the high volatility states do not depend on the series i, which significantly reduces the number of model parameters.

Finally, the stochastic cycle ψ is modeled as in Harvey and Trimbur (2003) where we set $q = 2$. By construction of the "cascading" stochastic cycle, we iterate through starting with $j = 1, ..., q$, where $j = 0$ is the cyclical noise:

$$\begin{bmatrix} \psi_{t+1}^{(j)} \\ \psi_{t+1}^{+(j)} \end{bmatrix} = \rho \begin{bmatrix} \cos\lambda & \sin\lambda \\ -\sin\lambda & \cos\lambda \end{bmatrix} \begin{bmatrix} \psi_t^{(j)} \\ \psi_t^{+(j)} \end{bmatrix} + \begin{bmatrix} \psi_t^{(j-1)} \\ \psi_t^{+(j-1)} \end{bmatrix} \tag{8}$$

$$\begin{bmatrix} \psi_t^{(0)} \\ \psi_t^{+(0)} \end{bmatrix} = \begin{bmatrix} \kappa_t \\ \kappa_t^{+} \end{bmatrix} \qquad \text{and} \qquad \begin{bmatrix} \kappa_t \\ \kappa_t^{+} \end{bmatrix} \sim N(0, \sigma_{t,\kappa}^2 I_2) \tag{9}$$

As for the trend and idiosyncratic cyclical components, the volatility $\sigma_{t,\kappa}^2$ is stochastic and time varying and follows equations (5) - (7) by removing dependence on an series index i and for $z = \kappa$. The coefficient ρ controls the width of the frequency band of the filter in the band pass filter representation.

In addition to parameters controlling stochastic volatilities $K_\eta^{(1)}$, $K_\varepsilon^{(1)}$ and $K_\kappa^{(1)}$ we estimate the drift parameter for the GDP, μ_3, set the drifts for PCE and unemployment rate at zero with $\mu_1 = 0$ and $\mu_2 = 0$, and estimate the parameters controlling the common cycle $\lambda \in (0, \pi)$, $\rho \in (-1, 1)$, $\xi_{i=2,3} \geq 0$, $\delta_{i=2,3}$. Further restrictions on ξ make its estimation difficult in order to satisfy the condition $-0.5\pi < \xi_i\lambda < 0.5\pi$ that directly depends on the parameter λ. As an alternative, we define a new parameter $\omega_i = \xi_i\lambda \in (-0.5\pi, 0.5\pi)$ that replaces ξ_i during the model estimation.

Similar to Creal et al. (2010) we do not estimate the probability of the regime switches p and set it to one of the values commonly found in the literature 3%, 5% and 10% due to data limitations and a short sample size. Most importantly, we allow for stochastic volatility in all studied series and estimate all parameters controlling the volatility of volatility in the high states for trend, cycle and idiosyncratic cyclical components.

3.2 Alternative Model Specifications

3.2.1 Multivariate Models

Our benchmark model, CKZ-SV, presented in Section 3.1, includes stochastic volatility for all studied series, which poses a question whether certain constraints might be beneficial in addressing potential overfitting in performing out-of-sample forecasts. Our model of choice restricts parameter $p = 0.03$ following Creal et al. (2010), since the parameter is only weakly identified using the short quarterly series available for the estimation.

The first alternative, called CKZ-UR (unrestricted CKZ) is directly based on the Creal et al. (2010) specification with stochastic volatility in the PCE and GDP series and with constant volatility for the unemployment series, hence setting up the restrictions $\sigma_{2,t,z}^2 = \sigma_{2,z}^2$ for $z \in \{\eta, \varepsilon\}$ in the CKZ-SV model. However, in contrast to Creal et al. (2010) who calibrate the parameters that control the volatility of volatility in $K_{i,t,z}$, we estimate these parameters.

The second alternative, which we refer to as CKZ is directly based on Creal et al. (2010)

specification with stochastic volatility in the PCE and GDP series and with constant volatility for the unemployment series. Volatility of volatility parameters $K_{i,t,z}$ in this model take the same values given in Creal et al. (2010): $K_{i,t,\varepsilon} = 0.05$, $K_{i,t,\eta} = 0.001$ for $i = 1, 3$, and $K_{t,\kappa} = 0.05$.

The third alternative, called MUC-SV-BP, is a version of the CKZ-SV model that imposes even further restrictions with stochastic volatility present only in the PCE series and in the common cyclical component. Finally, the fourth alternative, called MUC-BP assumes a common cyclical component with no stochastic volatility and constant volatility across all components for all studied series.

3.2.2 Univariate Models

In this study, we consider a variety of unobserved component (UC) models, first introduced by Harvey (1985) to decompose time-series data into cyclical and trend components using a Kalman filter, and generalized later to accommodate several salient features of the data. Among these extensions, we note the unobserved component model with stochastic volatility (UCSV) proposed by Stock and Watson (2007), the UC model with auto-regressive cyclical component (UC-0), and the UC model with both auto-regressive cyclical components and correlated innovations, the "unrestricted" UC model (UC-UR), developed by Morley, Nelson and Zivot (2003). Details of these models are available in the Appendix. In addition, we also present results for the univariate version of the CKZ model, the UC-BP model, that was first introduced by Harvey and Trimbur (2003). In the model each of the series is estimated in isolation and with no stochastic volatility.

Since each class of univariate models allows to account for different features of the data like stochastic volatility (UCSV), persistence of cyclical component (UC-0 or UC-UR), instantaneous correlation between trend and cycle innovations (UC-UR), or a band-pass based cycle (UC-BP) with a varying degree of parametrization, we also investigate if optimal model pooling improves forecasting performance. We follow model pooling introduced in Amisano and Geweke (2017) and dynamically change optimal model weights according to

$$\mathbf{w}_t = \text{argmax} \sum_{s=1}^{t} log \sum_{j=1}^{n} w_{t,j} p(y_{i,s}|y_i^{s-1}, M_j) \tag{10}$$

where $\mathbf{w}_t = \{w_{t,1}, \ldots, w_{t,n}\} \geq 0$, $\sum_{j=1}^{n} w_{t,j} = 1$, $n = 5$ is a number of univariate models in the pool, M_j is a jth univariate model, and $p(y_{i,t}|y_i^{t-1}, M_j)$ is a marginal likelihood evaluated at time t given model M_j. We discuss the evaluation of the marginal likelihood in the fully Bayesian context in the following Section 3.3.

3.3 Online Parameter Estimation and Forecasting

Since our models clearly fit into the state-space modeling framework, we use Bayesian estimation methods specifically designed to account for both parameter and state uncertainty. As shown in Section 4, addressing parameter uncertainty is an important feature that can significantly affect model ability for out-of-sample forecasts especially for the multivariate models. The reason for its importance stems from the relatively limited number of observations for macroeconomic variables with quarterly or monthly data frequencies that translate into higher parameter uncertainty the hence forecast uncertainty. However, due to computational difficulties, parameter uncertainty is rarely accounted for in the trend-cycle decomposition problems and the parameter estimation is frequently applied only once using all available observations. Such approach naturally imposes significant out-of-sample biases on the derived forecast evaluation measures.

In this paper we address both of these issues and perform an online estimation of parameters and states jointly. Recent advances in Bayesian literature and sequential Monte Carlo methods make such estimation feasible. In this work we utilize the SMC^2 online estimation algorithm of Chopin et al. (2013) and apply the PMCMC estimation method of Andrieu et al. (2010) to rejuvenate the filter particles. To initialize the estimation we use the batch estimation method of Duan and Fulop (2015), which proved to enforce stability when the total number of observations used is very small. The output from the SMC^2 algorithm consists of a sequence of filtered distributions of parameters and states approximated with M parameter particles with their respective weights $(\theta_t^{1:M}, w_{\Theta,t}^{1:M})$. For each of the m-th parameter particle with $m \in (1, \ldots, M)$, there are N associated state particles along with their respective weights $(x_t^{m,1:N}, w_t^{m,1:N})$. The SMC^2 method is summarized below as Algorithm 1.

We use the first 50 observations spanning dates from 1960:Q1 to 1972:Q1, which we treat as a training sample, to estimate all models using the Duan and Fulop (2015) method. Since the method provides the smoothed distribution of parameters and states, we use it as an input for the on-line estimation method of Chopin et al. (2013) for the rest of the sample up to 2023:Q2. We pick $M = 1024$ and $N = 8192$ to obtain a high degree of precision. Our forecasts are performed along with the iterations of the SMC^2 algorithm for $k \in \{1, 2, 4, 8\}$ quarters ahead. The forecast density for horizon k formulated at time t for model M_j is given as

$$p(y_{i,t+k}|y_i^t, M_j) =$$
$$\int_{\Theta^{(j)}} \int_x p(y_{i,t+k}|x_{i,t+k}, \theta_t^{(j)}) p(x_{i,t+k}|x_{i,t+k-1}, \theta_t^{(j)}) \cdots p(x_{i,t+1}|x_{i,t}, \theta_t^{(j)}) p(x_{i,t}|y_i^t, \theta_t^{(j)}) dp(\theta_t^{(j)}|y_i^t) \quad (11)$$

where the first integration is replaced by a finite sum over the time t filtered parameter particles, the second integration is replaced by a finite sum over the respective filtered and propagated particles up to time $t + k$ given the parameters. The dependence on model M_j is explicit through $\theta_t^{(j)}$ and

Algorithm 1 SMC^2 estimation algorithm for a joint state and parameter inference.

Require: Start at time $t = 0$ with M parameter parameter particles $\{\theta_t^m\}_{m\in(1,\dots,M)}$, each associated with N state particles $x_t^{m,1:N} \equiv \{x_t^{m,n}\}_{n\in(1:N)}$, $m \in (1,\dots,M)$. $f_{\theta_t^m}$ denotes the state evolution pdf and $g_{\theta_t^m}$ denotes the observation equation pdf for parameters θ_t^m.

for **do** $t \in (1,\dots,T)$
    for **do** $m \in (1,\dots,M)$
        for **do** $n \in (1,\dots,N)$
            sample $x_t^{m,n} \sim f_{\theta^m}(x_t \mid x_{t-1}^{m,n})$
            $w_t^{m,n} \leftarrow g_{\theta^m}(y_t \mid x_t^{m,n})$
        end for
        $x_t^{m,1:N} \sim \text{resample}(x_t^{m,1:N}, w_t^{m,1:N})$
        $\omega_{\Theta,t}^m \leftarrow \omega_{\Theta,t-1}^m \cdot \sum_{n=1}^N w_{\Theta,t}^{m,n}$
    end for

    if degeneracy condition for parameter weights $\omega_{\Theta,t}^{1:M} \equiv \{\omega_{\Theta,t}^m\}_{m\in(1:M)}$ is satisfied **then**
        $(\theta_t^{1:M}, x_t^{1:N,1:M}, w_t^{1:M,1:N}) \sim \text{rejuvenate}(\theta_t^{1:M}, x_t^{1:M,1:N}, w_t^{1:M,1:N})$
        $\omega_{\Theta,t}^{1:M} \leftarrow 1$
    end if
end for

its parameter support $\Theta^{(j)}$. It is important to note that our analysis differs significantly from that of Creal et al. (2010) since we formulate our forecasts with no look-ahead bias and re-estimate parameters at each time increment thanks to the SMC^2 pseudo-online estimation method discussed above.

3.4 Priors

The multivariate models that we study are richly parameterized. We impose priors along with restrictions on parameter supports in our estimation. The goal is to ensure stability and allow for maximum extraction of information content from the data in the estimation process. Thus, for some parameters we have fairly loose but informative priors, while for the rest the priors are practically uninformative, as shown in Table 1.

For the multivariate models, the parameter set, Θ, includes location, scale, and autocorrelation parameters. We picked uninformative log normal priors for scale parameters, $\sigma_{i,z}^2$ and K_z^2, where $z \in \{\varepsilon, \eta, \kappa\}$ and $i \in \{1, 2, 3\}$. For location parameters we imposed uninformative normal priors. For the models with a common cycle, we rescale parameters λ and ω_i by π. We define an uninformative beta prior for $\hat{\lambda}$ with a beta prior that imposes a mode length of business cycle corresponding to about 20 quarters periodicity. Finally, for the univariate models for the parameters common to the multivariate setting we pick the same priors. The uninformative priors for the parameters controlling the AR specification for UC-UR and UC-0 models are shown in the last two rows of Table 1.

Table 1: Priors for model parameters

			Models				
Param.	Distr.	Hyperparam.	CKZ-SV	CKZ-UR	MUC-SV-BP	MUC-BP	UC-UR
K_ε	Uniform	$(1e-5, 1)$	Y	Y	Y		
K_η	Uniform	$(1e-5, 1)$	Y	Y	Y		
K_κ	Uniform	$(1e-5, 1)$	Y	Y	Y		
$\sigma^2_{i,\varepsilon}$	lognormal	(0, 1)		Y: i=2	Y: i=2,3	Y: i=1,2,3	Y
$\sigma^2_{i,\eta}$	lognormal	(0, 1)		Y: i=2	Y: i=2,3	Y: i=1,2,3	Y
σ^2_κ	lognormal	(0, 1)				Y	
ρ	Uniform	(0, 0.99)	Y	Y	Y	Y	
$\hat{\lambda}$	Beta	(2.64, 15.06)	Y	Y	Y	Y	
μ_i	Normal	(1, 1)	Y: i=3	Y: i=3	Y: i=3	Y: i=3	Y
δ_i	Normal	(0, 1)	Y: i=2,3	Y: i=2,3	Y: i=2,3	Y: i=2,3	
$\hat{\omega}_i$	Uniform	$(1e-5, 1.5)$	Y: i=2,3	Y: i=2,3	Y: i=2,3	Y: i=2,3	
ϱ_i	Uniform	(-1, 1)					Y
ϕ_i	Uniform	(-1, 1)					Y

This table reports prior distributions imposed on the set of parameters in each estimated model. $\hat{\lambda} = \lambda/\pi$ and $\hat{\omega}_i = \omega_i/\pi$ are the scaled versions of λ and ω, respectively. The UC-SV and UC-UR models are discussed in the Appendix. The parameters for the UC-SV model overlap with the multivariate stochastic volatility models. The parameters for the univariate models should be estimated separately for each data set i.

What distinguishes our approach from that in Creal et al. (2010) is that we allow for a free estimation of parameters related to the volatility of volatility K_z, and do not impose an informative δ prior assuming their values. Hence, we directly account for additional source of parameter uncertainty present in the unrestricted versions of the model like CKZ-SV and CKZ-UR.

4 Empirical Findings

In this section, we summarize the empirical results from fitting the benchmark CKZ-SV model and alternative models to the data. We first discuss parameter estimates and informativness of priors for the benchmark model. We then compare forecasting results across estimated multivariate and univariate models estimated with either fully Bayesian or MLE methods. Finally, we compare trend-cycle decompositions stemming from the studied multivariate and univariate models.

4.1 CKZ-SV Benchmark Model Parameter Estimates

We discuss parameter estimates of the benchmark CKZ-SV model. Factor loadings $\delta_{i=2,3}$ filtered mean estimates, shown in the top panel of Figure 2, suggest that the dependence of GDP and UNRATE on the common cycle increased in time and almost tripled since the early 1970s. However, there are several instances of abrupt decrease in the factor loadings during crisis periods. The most notable decreases in the factor loadings can be associated with the GFC and COVID periods, where factor loadings sharply decreased by two- and three-fold, respectively. The sharp declines suggest that the changes in cyclical component were, in relative terms, mostly contributing to changes in PCE rather than GDP and UNRATE at these times.

Phase shift parameter $\xi_{i=2,3}$ filtered mean estimates are presented in the middle panel of Figure 2. The values of phase shift parameters represent leads (positive values) or lags (negative values) of the common cycle, measured in quarters, in explaining GDP (left chart) and UNRATE (right chart) with the phase shift set at 0 for PCE. Unlike the factor loadings, the phase shift parameters showed stable estimates through time with more abrupt changes present in the recessions (marked in grey). Similar to the factor loadings, the phase shift parameters for both GDP and UNRATE showed sharp declines during the GFC and COVID periods. The relation was close to instantaneous during the GFC period and instantaneous during the COVID period, rather than leading relative to PCE. A plausible explanation is a need to explain sharp PCE movements during the GFC and COVID periods by the common cycle that coincided with the movements in GDP and UNRATE. In other times, however, the common cycle affected GDP and UNRATE about two quarters before affecting PCE.

The last row of Figure 2 shows filtered mean estimates of parameter λ, $\hat{\lambda}$, further reparameterized as $2\pi/\hat{\lambda}$ to interpret the values as the typical length of the business cycle discussed in Section 3.1. The mid-length of business cycle showed an increasing trend from the 1970s up to the GFC, reaching values of about 75 quarters, and then from the GFC up to the COVID period, reaching values of about 110 quarters. Most notably, the mid-length of the common cycle dropped significantly during the GFC and the COVID periods. The drop can be explained by the common cycle property of explaining high-frequency jump events.

In Figure 3 we present prior distributions (dotted lines) and the full-sample posteriors for the CKZ-SV model. The top row presents the results for the volatility of volatility parameters $K_\eta^{(1)}$, $K_\varepsilon^{(1)}$ and $K_\kappa^{(1)}$, respectively. As seen in the charts, the posterior distributions differ substantially from the assumed uninformative priors supporting our claim that the volatility of volatility parameters can be efficiently estimated in our sample. Similarly, the parameters $\xi_{i=2,3}$ and $\delta_{i=2,3}$ governing the phase shift and factor loadings for GDP and UNRATE can be estimated with precision using uninformative priors. The same holds true for the parameter controlling the width of the frequency band of the common cycle.

Figure 2: Filtered Posterior Means of Common Cycle Parameters

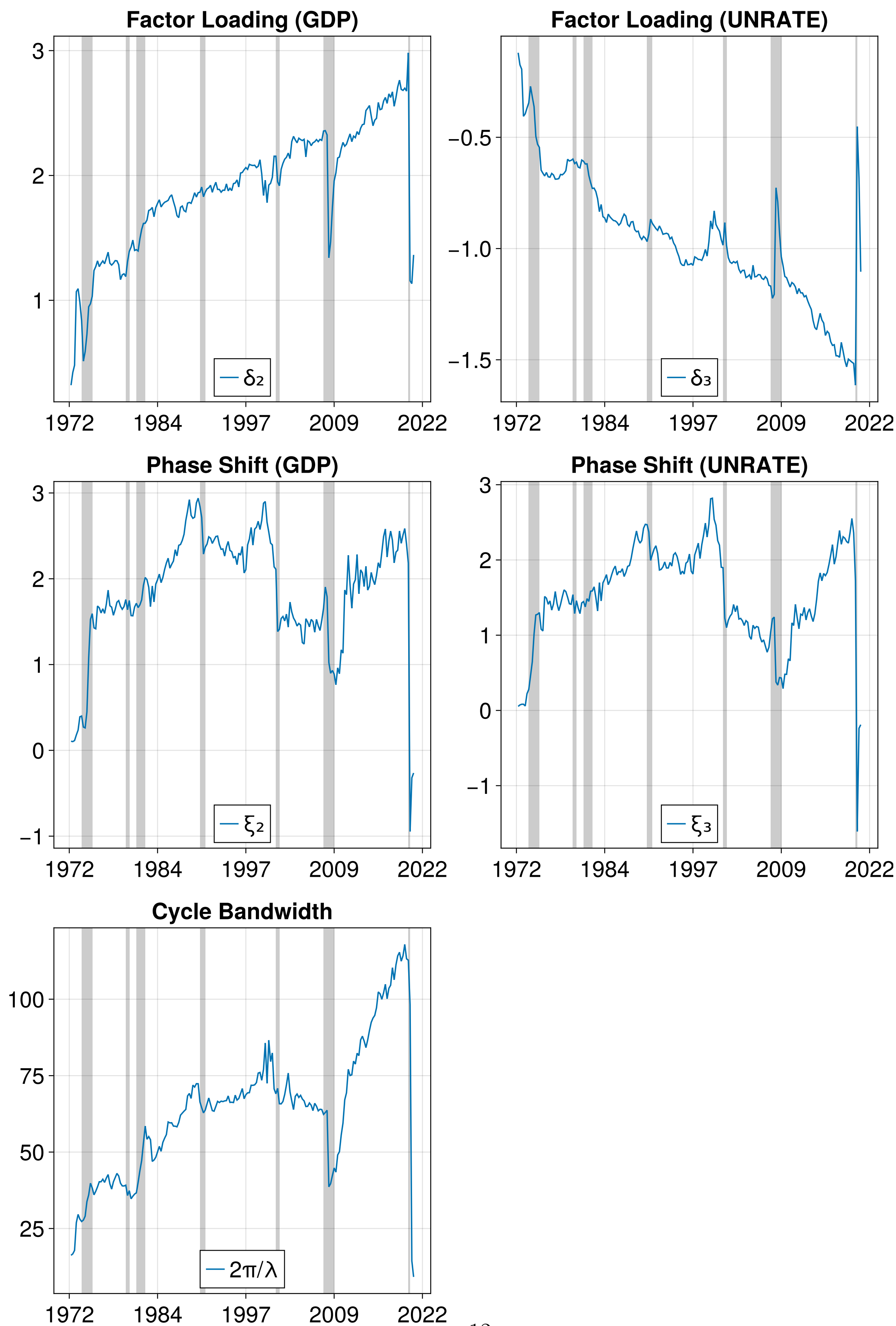

Figure 3: Prior and posterior distributions of estimated parameters for the benchmark model

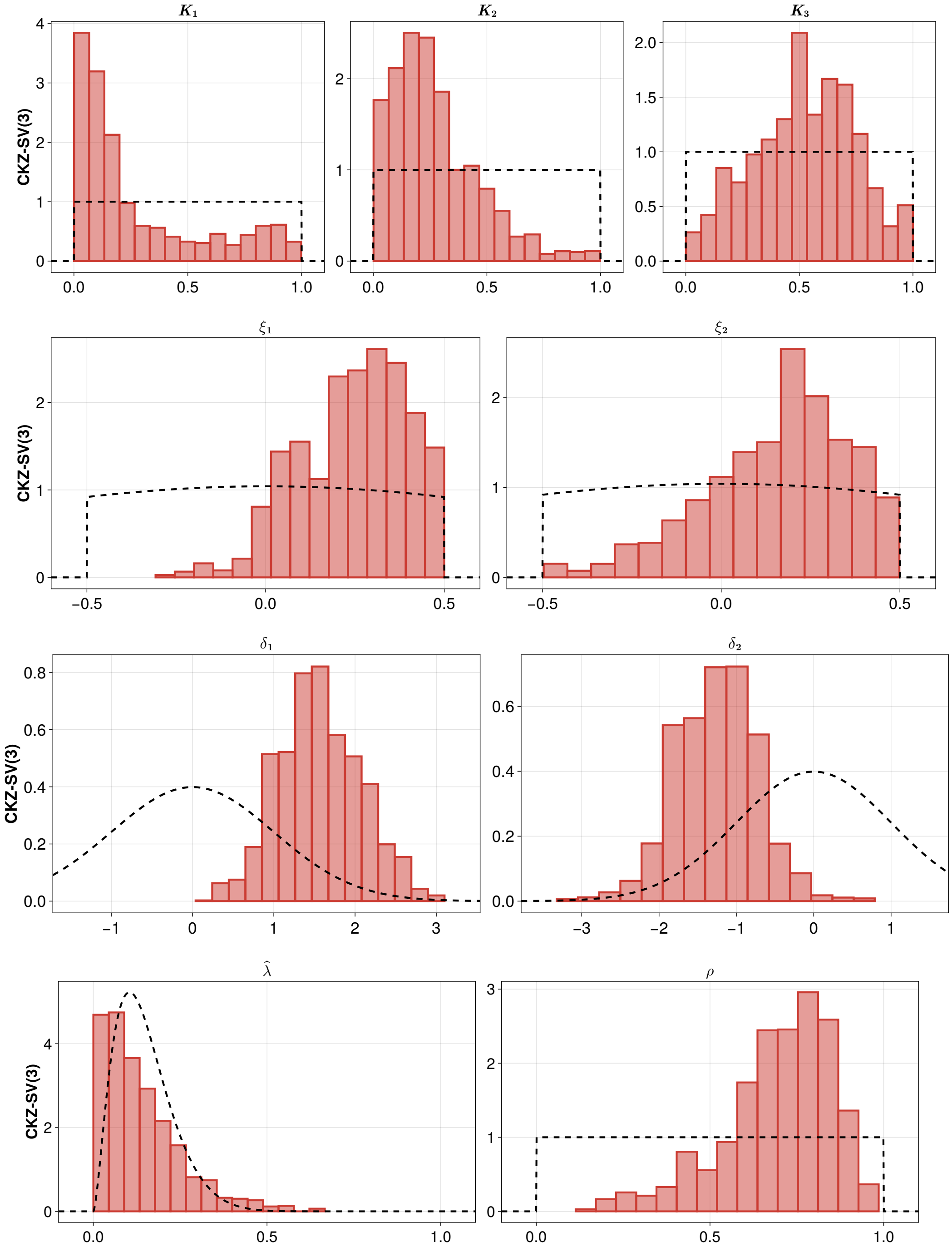

The dashed lines represent the prior distributions for estimated parameters, while the histograms represent the porterior distributions. All results are based on 1024 parameter draws. Cloud sizes are $M = 1024$ and $N = 8192$, representing outside and state clouds, respectively.

4.2 Comparison of Forecasting Performance

4.2.1 Forecasting Performance of Multivariate Models

Panel A in Table 2 reports fully Bayesian root mean squared forecast errors (RMSFE) for PCE, UNRATE, and GDP based on SMC^2 algorithm and online forecasting paradigm, for forecast horizons $k = 1, \ldots, 8$, across all multivariate models described in Sections 3.1 and 3.2.1.

Table 2: Root Mean Squared Forecast Errors: multivariate models

		Panel A: SMC^2 estimation, with parameter uncertainty				
	k	CKZ-SV	CKZ-UR	CKZ	MUC-BP-SV	MUC-BP
PCE	1	1.8590	1.8712	1.9849	1.9204	2.1381
	2	2.0505	2.0531	2.2283	2.1194	2.5338
	4	2.2665	2.3075	2.4928	2.4815	3.3841
	8	2.6621	2.6714	2.8154	2.9127	4.9543
UNRATE	1	0.6012	0.5630	0.5617	0.5578	0.7339
	2	0.8007	0.8453	0.8215	0.8522	1.1691
	4	1.1824	1.2661	1.2413	1.2935	1.8716
	8	1.6501	1.7106	1.7172	1.7793	2.8217
GDP	1	0.9484	1.1047	0.9849	1.1151	1.3456
	2	1.4140	1.6837	1.4725	1.6630	1.9664
	4	2.1615	2.5870	2.2881	2.5192	3.0117
	8	3.3047	3.7507	3.5019	3.6391	4.5975
		Panel B: MLE Estimation, no parameter uncertainty				
PCE	1	2.0060	1.9331	2.0133	1.9747	2.1176
	2	2.1254	2.0716	2.2402	2.1641	2.4659
	4	2.3455	2.3214	2.5215	2.5444	3.1955
	8	2.8810	2.7879	2.8129	2.9463	4.5274
UNRATE	1	0.6694	0.5825	0.5698	0.5973	0.6976
	2	0.8354	0.7961	0.8074	0.8925	1.0536
	4	1.1793	1.1997	1.1992	1.3350	1.5995
	8	1.7312	1.6705	1.5942	1.8331	2.7121
GDP	1	1.0838	1.0383	1.0065	1.1917	1.2527
	2	1.5418	1.5953	1.5374	1.7497	1.7518
	4	2.4188	2.5409	2.4164	2.6765	2.5780
	8	4.0756	4.1354	3.8279	4.0695	4.2092

The table shows the root mean squared forecast errors for models estimated with the SMC^2 method that acounts for parameter uncertainty (Panel A) and estimated with the MLE method with no parameter uncertainty (Panel B). The results are presented for all considered multivariet specifications discussed in Section 3.2.1 and for all studied macroeconomic series of PCE, UNRATE and GDP.

Starting with PCE results in Table 2, we notice that our benchmark CKZ-SV model yields forecast improvements compared to the baseline CKZ, and all other multivariate models across all forecast horizons. We note that while the benchmark CKZ-SV model outperforms the CKZ-UR model, RMSFEs of these two models are very close for PCE forecasts. Since equation (7) imposes the same restrictions on all three variables, this may force the CKZ-SV and CKS-UR estimations to be close, resulting in no apparent gains from spillovers from UNRATE volatility of volatility to other variables. In comparison to other multivariate models, CKZ-SV clearly and unambiguously yields better forecasts.

We next turn to UNRATE forecast results. The benchmark CKZ-SV model dominates other multivariate models and yields smaller RMSFEs for $k = 2, \ldots, 8$. For $k = 1$, CKZ-UR, CKZ, and MUC-BP-SV models outperform the benchmark slightly. Finally, for GDP the benchmark CKZ-SV model yields smaller RMSFEs compared to all other multivariate models studied and across all forecast horizons.

We notice that the relative performance (in terms of RMSFE) of the benchmark CKZ-SV compared to other models, especially the baseline CKZ model, generally improves as k increases. This observation generally holds across all three variables considered. Parameter uncertainty induces fatter tails in forecast densities for variables. We believe that the benchmark model, given the presence of the stochastic volatility components and the resulting additional flexibility, is better suited to handle draws from such regions as forecast horizon increases, helping in higher forecast precision.

In Panel B of Table 2, we report the RMSFEs based on full information maximum likelihood estimations for all time t for the same models studied in Panel A. In this exercise, there is no parameter uncertainty by construction, and the point estimates of parameters are used. When comparing RMSFEs across models and forecast horizons k in Panels A and B, it is easy to see that MLE-based RMSFEs are generally much larger than their SMC^2 counterparts. In particular, fully Bayesian benchmark CKZ-SV model RMSFEs are uniformly smaller than their MLE counterparts, and by a wide margin. This pattern holds for other multivariate models when forecasting PCE and UNRATE. There two exceptions for GDP: CKZ-UR (only for smaller forecast horizons) and MUC-BP maximum likelihood-based RMSFEs are smaller than their fully Bayesian counterparts. The fact that MUC-BP does not feature a stochastic volatility component and the unrestricted nature of CKZ-UR (thus, a relatively higher burden to identify dynamics from a relatively smooth variable) are likely to contribute to these results.

In addition, we present in the Appendix alternative CKZ-SV(p) model forecasting results for different values of parameter p that was set at 3% in the benchmark model (we use CKZ-SV(3) and CKZ-SV notation interchangeably). While, in general, the CKZ-SV(3) benchmark model performs overall best for UNRATE and GDP series, it can potentially further be improved by choosing a higher probability of high volatility of volatility states for PCE with the best performance for 10% level. We leave further improvements of the CKZ-SV specification for future research.

4.2.2 Forecasting Performance of Univariate Models

In Table 3 we report RMSFEs for all univariate results discussed in Section 3.2.2. It is immediately clear that except for two cases where forecast horizon is $k = 8$, the UC-SV model yields the lowest RMSFEs across all three variables and forecast horizons. Thus, it appears that including a stochastic volatility component in the standard Harvey (1985) and Stock and Watson (2007) UC model, materially improves it's forecast ability for important macroeconomic variables.

Table 3: Root Mean Squared Forecast Errors: univariate models

		Panel A: SMC^2 estimation, with parameter uncertainty					
	k	UC	UC-0	UC-UR	UC-BP	UC-SV	Pool
PCE	1	1.9170	1.9451	1.9397	1.9187	1.8748	1.8652
	2	2.0707	2.1022	2.0939	2.0731	2.0294	2.0254
	4	2.3731	2.3954	2.3894	2.3582	2.3208	2.3159
	8	2.6440	2.6784	2.6720	2.5977	2.8105	2.6096
UNRATE	1	0.6454	0.6372	0.7076	0.6733	0.6614	0.5951
	2	0.9324	0.9218	1.0558	0.9930	0.8806	0.8579
	4	1.3647	1.3455	1.5556	1.4181	1.2695	1.2774
	8	1.9464	1.9040	2.2204	1.8707	1.8329	1.8858
GDP	1	1.1572	1.1460	1.1999	1.2173	1.1740	1.0361
	2	1.6411	1.6371	1.6882	1.7892	1.6331	1.5027
	4	2.4608	2.4704	2.5100	2.8513	2.4562	2.3119
	8	3.6895	3.7234	3.6989	4.5607	3.8729	3.6179
		Panel B: MLE Estimation					
PCE	1	1.9160	1.9406	1.9401	1.9267	1.8762	1.8662
	2	2.0697	2.1044	2.0984	2.0905	2.0302	2.0271
	4	2.3770	2.3982	2.3967	2.3349	2.3312	2.3166
	8	2.6409	2.6910	2.6897	2.5096	2.6095	2.5126
UNRATE	1	0.6381	0.6356	0.7189	0.6715	0.6951	0.5791
	2	0.9251	0.9200	1.0794	0.9908	0.8997	0.8376
	4	1.3589	1.3460	1.5965	1.4261	1.2730	1.3538
	8	1.9444	1.9101	2.2630	1.8818	1.8249	1.9094
GDP	1	1.1395	1.1403	1.1876	1.2084	1.1617	1.0095
	2	1.6195	1.6268	1.7002	1.7635	1.6301	1.5015
	4	2.4310	2.4615	2.5889	2.7812	2.4587	2.4098
	8	3.6403	3.7222	3.8481	4.3969	3.9385	3.7143

This table reports fully Bayesian root mean squared forecast errors, based on SMC^2 algorithm, for univariate models introduced in Section 3.2.2. The column labeled as "Pool" reports RMSFE for optimally pooled combinations of all estimated univariate models, closely following Amisano and Geweke (2017).

Among others, Amisano and Geweke (2017) have shown that univariate forecasts of macroeconomic variables could be improved by optimally pooling forecasts of many models, as described in Section 3.2.2. The final column in the table reports RMSFE for such optimally pooled forecasts. We note that these optimal pooled forecasts consistently yield RMSFEs that are smaller than the best individual univariate models' RMSFEs. Based on the evidence from studies such as Andreou et al. (2013) and Jahan-Pavar and Lang (2024), we know that in a simple model averaging exercise, the averaged RMSFEs are not necessarily smaller than all estimated models, but they are more stable. In other words, for a sample $\{y_{i,t}\}_{t=1}^{T}$, there exists a "best" model that outperforms the averaged forecast in terms of RMSFE, while we do not observe a similar pattern for optimally pooled Bayesian forecasts.

The superior performance of optimally pooled forecasts (compared to optimally averaged forecasts) stems from the way that univariate models receive a weight in optimal pooling exercises. Figure 4 reports the weights assigned to each univariate model. As expected, the UC-SV model typically receives a high optimal weight in the pooling procedure, closely followed by the UC-UR model of Kamber et al. (2018) and the UC-BP model of Harvey and Trimbur (2003). These are extreme-case models: UC-UR allows for correlation between trend and cyclical components of the variable, while the flexibility of the band-pass UC-BP admits dynamic adjustment of frequency bands associated with the cyclical component.

In contrast to the multivariate estimation results reported in Table 2, the difference between fully Bayesian (Panel A in Table 3) and full-information maximum-likelihood (Panel B in Table 3) estimations of univariate model do not yield significantly different RMSFEs. The closeness of these results could be partially due to the small number of parameters to be estimated in univariate models, and thus higher precision of estimation and thus less impact from accounting for parameter uncertainty.

4.3 Comparing trend-cycle decomposition results

As shown in Figure 1, the CBO estimates of output gap and cyclical unemployment fall within the 95 percent credible intervals of the cyclical components that we recover from applying the benchmark CKZ-SV model to the data. In comparison to a recent study by Barigozzi and Luciani (2023), our estimates do not point to a sustained positive output gap between 1999 and 2008. As with CBO and González-Astudillo (2019a) estimates, we find two positive output gaps in this time interval: one between mid-1990s and the 2001 recession, and the other between mid-2000s and 2008. In terms of magnitude, both are smaller than Barigozzi and Luciani (2023) estimates. That said, Figure 5 shows that among all multivariate models considered in our study, CKZ-SV yields cyclical components (output gaps and unemployment gaps) that are closer to Barigozzi and Luciani (2023).

Alternative models considered in our study yield output and unemployment gaps that differ markedly from CKZ-SV-based measures (see Figure 5), and are notably different from both CBO estimates and findings of studies such as Barigozzi and Luciani (2023). Alternative output (unemployment) gaps typically tend to dip (peak) more than the benchmark model in downturns, peak (dip) less in upturns, and rise (fall) much slower in expansions. As a result, these gaps typically underestimate (overestimate) positive (negative) output (unemployment) gaps compared to the benchmark CKZ-SV model. In comparison to the benchmark model, they generate relatively deep

Figure 4: Weights of univariate models in the forecast combination exercise

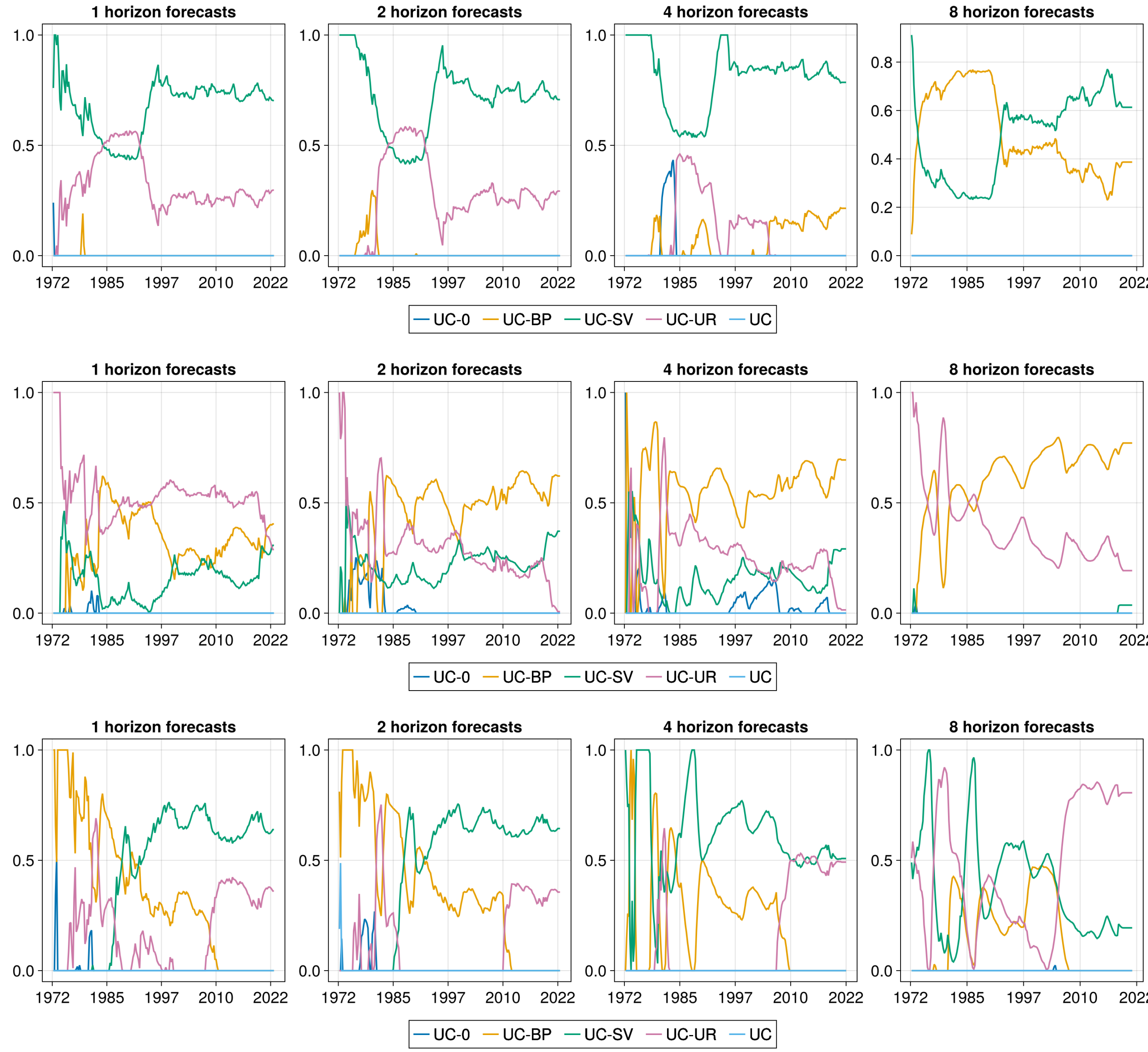

The figure reports the evolution of weights assigned to each univariate model used in the forecast combination exercise described in Section 4.2.2. The top row shows results for PCE, the middle row for UNRATE and the bottom row for GDP series.

negative output gaps and relatively large positive unemployment gaps. However, the behavior of alternative models yields counter-intuitive results during the COVID-19 pandemic when alternative models showed much smaller unemployment gaps implying inability to capture the abrupt turns in macroeconomic variables' trends. Thus, if employed as policy tools, the failures of these alternative models could have serious implications. This observation validates and reinforces our earlier conclusions about the crucial importance of incorporating time-variation in volatility and careful

Figure 5: Comparison of trend-cycle decomposition of variables across multivariate models

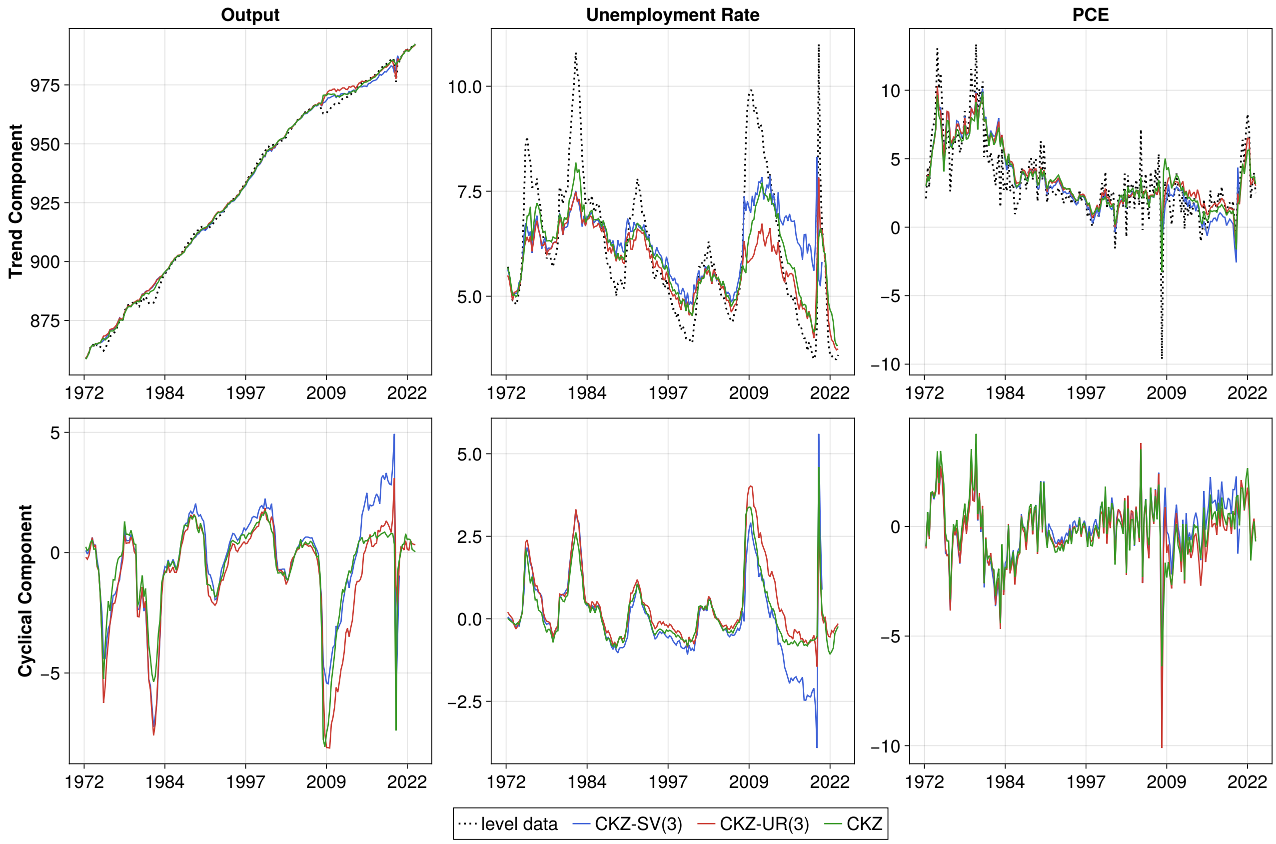

The top row reports the data and extracted stochastic trends for three multivariate models studied in this paper. The bottom row does the same for the extracted cyclical components. The details of modeling choices are available in Section 3.1 and Section 3.2.1.

modeling of feedback channels and dependencies between macroeconomic variables.

We now compare the trend-cycle decomposition of the data based on the univariate models discussed in Sections 3.2.2 and 4.2.2 with the benchmark model. Figure 6 displays these comparisons. It is immediately clear that output and unemployment gaps generated by the univariate methods severely underestimate peaks and troughs of the gap measures, both compared to the benchmark CKZ-SV model and to CBO estimates. The representative univariate methods displayed in Figure 6 are the UC-SV model of Stock and Watson (2007) and the UC-O model of Morley (2011). This comparison validates and reinforces our earlier conclusions about the crucial importance of using multivariate models and careful modeling of feedback channels and dependencies between macroeconomic variables.

Figure 6: Comparison of trend-cycle decomposition of variables across univariate models

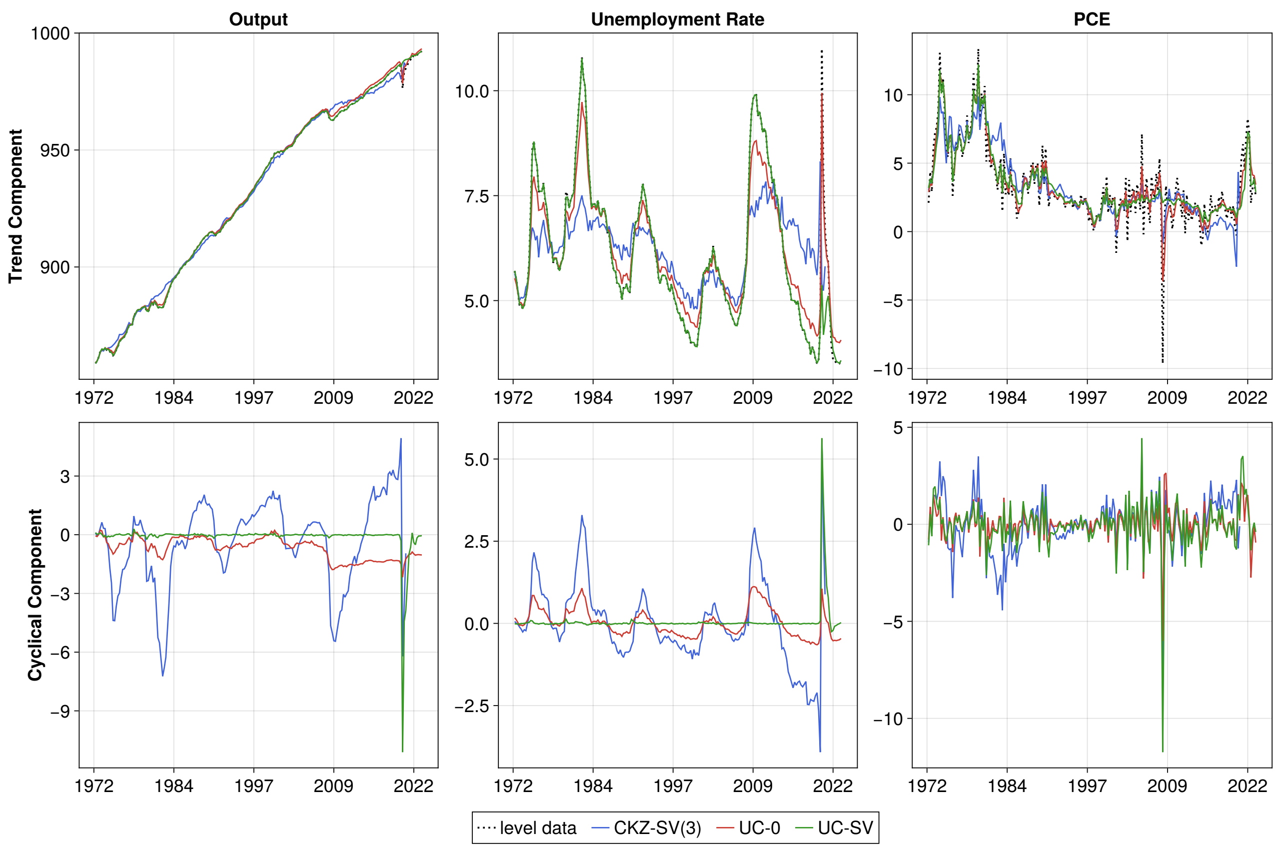

The top row reports the data and extracted stochastic trends for the benchmark multivariate model and two univariate models studied in this paper. The bottom row does the same for the extracted cyclical components. The details of modeling choices are available in Section 3.2.2 and the Appendix.

5 Conclusion

In this study, we propose a generalized multivariate unobserved component model to decompose and forecast U.S. output, unemployment, and inflation jointly. We expand and refine the multivariate unobserved components model proposed by Creal et al. (2010), by incorporating fully estimated SV components to induce estimation and forecasting flexibility–especially over periods of abrupt change, such as the COVID-19 pandemic–in all time series. The study exploits the capabilities of Chopin et al. (2013) SMC^2 method and perform online forecasting. We document that the fully Bayesian estimation, accounting for both parameter and state uncertainty, consistently dominates forecasts produced by many alternative multivariate (such as Creal et al., 2010) and univariate (such as Stock and Watson, 2007 and Kamber et al., 2018) models. Moreover, using a filtering approach avoids the look-ahead bias problems inherent in smoother-based estimation (as in Li and Koopman, 2021), that use the full sample. In addition, we show that when using univariate models, an optimally pooled model (following Amisano and Geweke, 2017) outperforms individual constituent models.

Our study explicitly incorporates relevant stylized facts about the United States macroeconomic data (comovements, nonstationarity, and the slow drift in long-run output growth over time). However, our method is a general estimation method suitable for various macroeconomic and financial time-series estimation, and is not tightly tailored and constrained for the specific application presented in the paper.

References

Amisano, G., Geweke, J., 2017. Prediction using several macroeconomic models. The Review of Economics and Statistics 99, 912–925.

Andreou, E., Ghysels, E., Kourtellos, A., 2013. Should macroeconomic forecasters use daily financial data and how? Journal of Business & Economic Statistics 31, 240–251.

Andrieu, C., Doucet, A., Holenstein, R., 2010. Particle Markov Chain Monte Carlo Methods. Journal of the Royal Statistical Society Series B (Statistical Methodology) 72, 269–342.

Barigozzi, M., Luciani, M., 2023. Measuring the Output Gap using Large Datasets. The Review of Economics and Statistics 105, 1500–1514.

Baxter, M., King, R.G., 1999. Measuring business cycles: Approximate band-pass filters for economic time series. the Review of Economics and Statistics 81, 575–593.

Beveridge, S., Nelson, C.R., 1981. A new approach to decomposition of economic time series into permanent and transitory components with particular attention to measurement of the 'business cycle'. Journal of Monetary Economics 7, 151 – 174.

Chopin, N., Jacob, P.E., Papaspiliopoulos, O., 2013. SMC^2: An efficient algorithm for sequential analysis of state-space models. Journal of the Royal Statistical Society: Series B (Statistical Methodology) 75, 397–426.

Clark, T.E., 2011. Real-time density forecasts from bayesian vector autoregressions with stochastic volatility. Journal of Business & Economic Statistics 29, 327–341.

Creal, D., Koopman, S.J., Zivot, E., 2010. Extracting a robust U.S. business cycle using a time-varying multivariate model-based bandpass filter. Journal of Applied Econometrics 25, 695–719.

Dobrev, D., Hansen, D., Szerszen, P., 2022. A randomized missing data approach to robust filtering and forecasting. URL: `https://arxiv.org/abs/2104.14664`, `arXiv:2104.14664`.

Duan, J.C., Fulop, A., 2015. Density-Tempered Marginalized Sequential Monte Carlo Samplers. Journal of Business & Economic Statistics 33, 192–202.

González-Astudillo, M., 2019a. Estimating the U.S. output gap with state-level data. Journal of Applied Econometrics 34, 795–810.

González-Astudillo, M., 2019b. An output gap measure for the euro area: Exploiting country-level and cross-sectional data heterogeneity. European Economic Review 120, 103301.

Grant, A.L., Chan, J.C., 2017. A Bayesian Model Comparison for Trend-Cycle Decompositions of Output. Journal of Money, Credit and Banking 49, 525–552.

Hamilton, J.D., 2018. Why you should never use the hodrick-prescott filter. the Review of Economics and Statistics 100, 831–843.

Harvey, A.C., 1985. Trends and cycles in macroeconomic time series. Journal of Business & Economic Statistics 3, 216–227.

Harvey, A.C., Trimbur, T.M., 2003. General model-based filters for extracting cycles and trends in economic time series. the Review of Economics and Statistics 85, 244–255.

Hodrick, R.J., Prescott, E.C., 1997. Postwar U.S. Business Cycles: An Empirical Investigation. Journal of Money, Credit and Banking 29, 1–16.

Jahan-Pavar, M.R., Lang, W.J., 2024. Which daily equity returns improve output forecasts? Economics Letters 243, 111897.

Justiniano, A., Primiceri, G.E., Tambalotti, A., 2013. Is there a trade-off between inflation and output stabilization? American Economic Journal: Macroeconomics 5, 1–31.

Kamber, G., Morley, J.C., Wong, B., 2018. Intuitive and Reliable Estimates of the Output Gap from a Beveridge-Nelson Filter. The Review of Economics and Statistics 100, 550–566.

Li, M., Koopman, S.J., 2021. Unobserved components with stochastic volatility: Simulation-based estimation and signal extraction. Journal of Applied Econometrics 36, 614–627.

Morley, J.C., 2011. The two interpretations of the beveridge-nelson decomposition. Macroeconomic Dynamics 15, 419–439.

Morley, J.C., Nelson, C.R., Zivot, E., 2003. Why Are the Beveridge-Nelson and Unobserved-Components Decomposition of GDP so Different? the Review of Economics and Statistics 85, 235–243.

Panovska, I., Ramamurthy, S., 2022. Decomposing the output gap with inflation learning. Journal of Economic Dynamics and Control 136, 104327.

Shackleton, R., 2018. Estimating and Projecting Potential Output Using CBO's Forecasting Growth Model. Technical Report Working Paper 2018-03. Congressional Budget Office. Washington, D.C.

Stock, J.H., Watson, M.W., 2007. Why Has U.S. Inflation Become Harder to Forecast? Journal of Money, Credit and Banking 39, 3–33.

Appendix

Univariate State-Space Models

UC and UCSV Models

The UC model of Harvey (1985) decomposes a time series into the trend component, x_t, driven by permanent shocks, and a cyclical component, η_t, driven by transitory shocks. The UCSV model of Stock and Watson (2007) further extends the UC specification by adding stochastic volatility components to the trend and the cycle. The UCSV model for a time series i can be defined as:

$$
\begin{aligned}
y_{i,t} &= x_{i,t} + \eta_{i,t} \\
x_{i,t} &= \mu_i + x_{i,t-1} + \varepsilon_{i,t} \\
\eta_{i,t} &\sim N\left(0, \sigma^2_{i,t,\eta}\right) \\
\varepsilon_{i,t} &\sim N\left(0, \sigma^2_{i,t,\varepsilon}\right) \\
\log \sigma^2_{i,t,\eta} &\sim N\left(\log \sigma^2_{i,t-1,\eta}, K^2_{i,\eta}\right) \\
\log \sigma^2_{i,t,\varepsilon} &\sim N\left(\log \sigma^2_{i,t-1,\varepsilon}, K^2_{i,\varepsilon}\right)
\end{aligned}
$$

for $t = 1, \ldots, T$, where $y_{i,t}$ is the decomposed time-series, and where $\sigma_{i,t,\eta}$ and $\sigma_{i,t,\varepsilon}$ are the stochastic volatility components of the trend and the cycle, respectively. The parameters $K_{i,\varepsilon} > 0$ and $K_{i,\eta} > 0$ control volatility of volatility. The innovations propagating stochastic volatility are mutually and serially independent. The standard UC model does not include stochastic volatility components and uses the restrictions $\sigma^2_{i,t,\eta} = \sigma^2_{i,\eta}$ and $\sigma^2_{i,t,\varepsilon} = \sigma^2_{i,\varepsilon}$ to impose time-invariant volatilities. The parameters ($K^2_{i,\varepsilon}$, $K^2_{i,\eta}$) and the parameters ($\sigma^2_{i,\eta}, \sigma^2_{i,\varepsilon}$) for the UCSV and UC models, respectively, are unknown and estimated.

UC-UR and UC-0 Models

Morley et al. (2003) propose the unrestricted unobserved component (UC-UR) model to reconcile differences in trend-cycle decomposition of real GDP implied by the UC model and Beveridge and Nelson (1981) approach. The UC-UR model allows for autocorrelated cyclical components. It also introduces correlations between innovations for trend and cycle components. The following state-space specification characterizes the UC-UR trend-cycle decomposition for a time-series i:

$$
\begin{aligned}
y_{i,t} &= x_{i,t} + \eta_{i,t} \\
x_{i,t} &= \mu_i + x_{i,t-1} + \varepsilon_{i,t} \\
\eta_{i,t} &\sim N\left(\phi_{i,1}\eta_{i,t-1}, \sigma^2_{i,\eta}\right) \\
\varepsilon_{i,t} &\sim N\left(0, \sigma^2_{i,\varepsilon}\right) \\
\varrho_i &= corr(\varepsilon_{i,t}, \eta_{i,t} - \phi_{i,1}\eta_{i,t-1})
\end{aligned}
$$

where the overlapping notation matches the preceding section. The parameter $\varrho_i \in (-1, 1)$ controls the correlation between innovations of trend and cycle components. The parameter ϕ_1 induces autocorellation in the cyclical component and satisfy the stationarity condition $|\phi_{i,1}| < 1$. The UC-0 model is a constrained version of UC-UR, where $\varrho_i = 0$.

Multivariate Models: Probability of High Volatility States

Table 4: Root Mean Squared Forecast Errors and Probability of High Volatility States

		MUC-SV-BP			CKZ-UR			CKZ-SV		
	k	0.03	0.05	0.10	0.03	0.05	0.10	0.03	0.05	0.10
PCE	1	1.9204	2.0228	1.8716	1.8712	1.8526	1.8527	1.8590	1.8569	1.8389
	2	2.1194	2.1991	2.0324	2.0531	2.0397	2.0121	2.0505	2.0419	1.9994
	4	2.4815	2.6989	2.2785	2.3075	2.2620	2.2423	2.2665	2.2939	2.2239
	8	2.9127	3.5445	2.5842	2.6714	2.6438	2.5968	2.6621	2.7933	2.6585
UNRATE	1	0.5578	0.5735	0.8228	0.5630	0.5363	0.5466	0.6012	0.5506	0.5870
	2	0.8522	0.8733	1.1994	0.8453	0.7983	0.7960	0.8007	0.7829	0.7748
	4	1.2935	1.4145	1.5082	1.2661	1.2253	1.1996	1.1824	1.2108	1.1581
	8	1.7793	2.5100	1.7248	1.7106	1.7265	1.6589	1.6501	1.7683	1.6423
GDP	1	1.1151	1.1799	1.6471	1.1047	0.9778	0.9487	0.9484	0.9630	0.9332
	2	1.6630	1.7503	2.2205	1.6837	1.4900	1.4833	1.4140	1.4858	1.4572
	4	2.5192	2.9118	2.8134	2.5870	2.3227	2.3427	2.1615	2.3083	2.3220
	8	3.6391	5.2008	3.6038	3.7507	3.4372	3.6489	3.3047	3.4018	3.5981

The table shows the root mean squared forecast errors for models estimated with the SMC^2 method across different values of paramater p in equation (7). The results are presented for multivariate specifications discussed in Section 3.2.1 and for all studied macroeconomic series of PCE, UNRATE and GDP.

CKZ-UR Model Parameter Full-Sample Posteriors

Figure 7: Prior and posterior distributions of estimated parameters for the unrestricted Creal, Koopman and Zivot (2010) model.

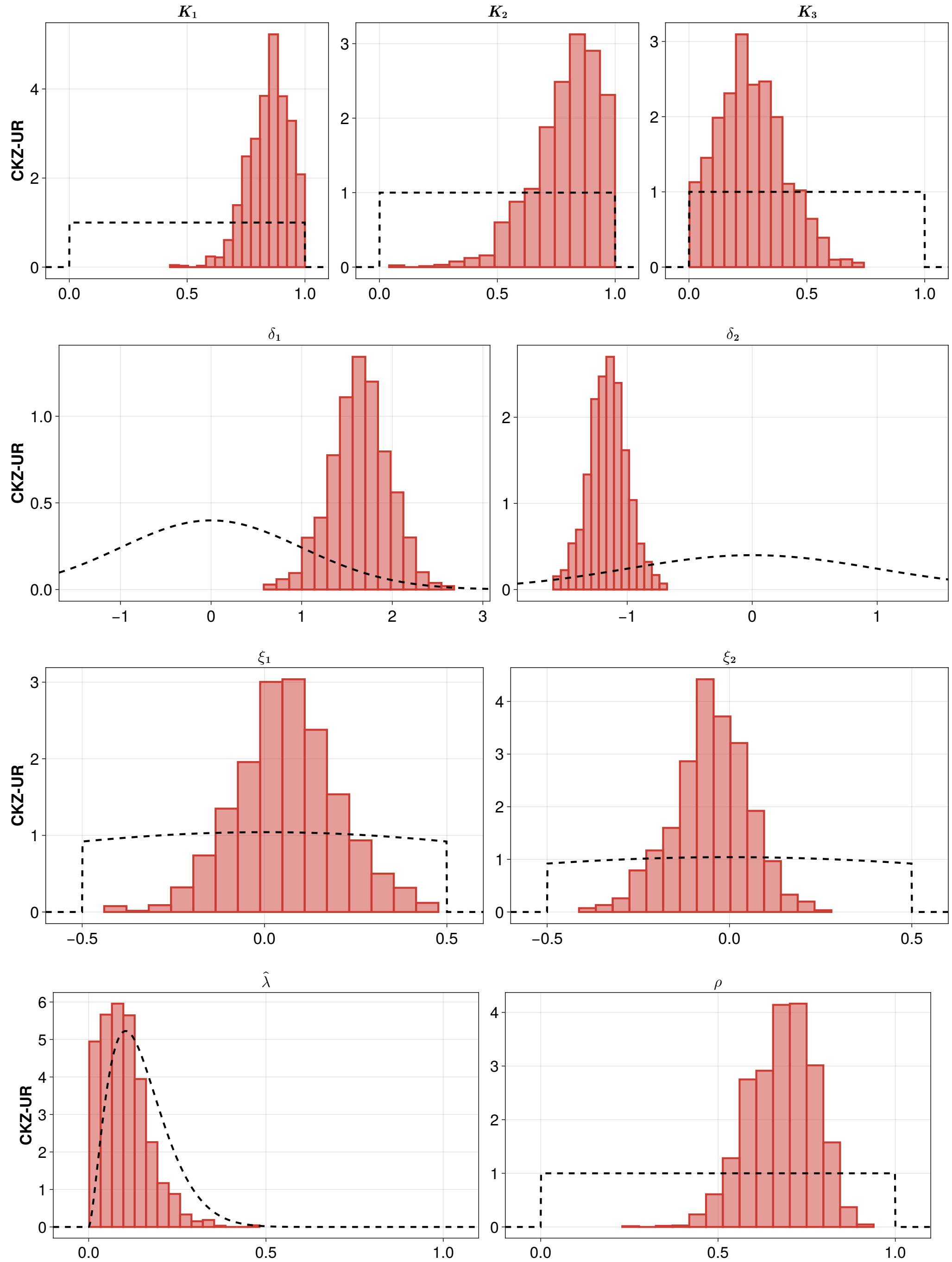

The dashed lines represent the prior distributions for estimated parameters, while the histograms represent the porterior distributions using all observations. Cloud sizes are $M = 1024$ and $N = 8192$.